Cell Research

LETTER TO THE EDITOR

piRNA 3′ uridylation facilitates the assembly of MIWI/piRNA complex for efficient target regulation in mouse male germ cells

Cell Research (2022) 32:1030–1033; https://doi.org/10.1038/s41422-022-00659-1

Dear Editor,

RNA tailing, i.e., addition of non-templated nucleotides to the 3′ end of RNAs, represents one of the most frequent RNA modifications that participate in regulation of RNA processing, function, degradation, etc.[1] PIWI-interacting RNAs (piRNAs) are a class of animal germline-specific small non-coding RNAs that guide PIWI proteins to suppress transposable elements and regulate protein-coding genes in germ cells, playing indispensable roles in germline development and fertility in animals.[2] 3′ terminal trimming and subsequent 2′-*O*-methylation are essential for piRNA processing and maturation, which are catalyzed by 3′-to-5′ exoribonuclease PNLDC1 and HEN methyltransferase 1 (HENMT1) in mice, respectively.[2] Most recently, a study reports that loss of 3′ terminal trimming and 2′-*O*-methylation induces non-templated RNA tailing on piRNA precursors and in turn triggers pre-piRNA decay, thereby severely interfering with piRNA production in worms.[3] However, whether and how RNA tailing is required for piRNA functions remains largely unclear. Here, we discovered that mouse PIWIL1 (MIWI)-bound piRNAs undergo non-templated RNA tailing and further showed the functional requirement of 3′ uridylation for the targeting efficacy of MIWI/piRNAs in mouse male germ cells, uncovering an unprecedented role for 3′ tailing in piRNA functions in mouse male germ cells.

By re-analyzing the anti-MIWI RIP-seq datasets that we previously generated in wild-type mouse testes,[4,5] we surprisingly found that >20% of MIWI-bound piRNAs failed to align to the mouse genome; however, these piRNAs became fully matched to the genome if removing one or several nucleotides at their 3′ end (Fig. 1a, b; Supplementary information, Table S1). This strongly indicates that non-templated RNA tailing also normally occurs on MIWI-bound mature piRNAs (hereafter referred to as tailed-piRNAs) in addition to abnormally occuring on piRNA precursors upon loss of 3′ terminal trimming and 2′-*O*-methylation in worms.[3] We further found that both tailed- and untailed-piRNAs were derived from the same genomic loci and shared similar species (Supplementary information, Fig. S1a, b), while the frequency of a specific tailed-piRNA was positively correlated with the piRNA abundance (Supplementary information, Fig. S1b). This suggests that 3′ tailing occurs on MIWI-bound piRNAs in a sequence-independent manner. Together, these results indicate the presence of 3′ tailing on a portion of MIWI-bound piRNAs in mouse testes.

Interestingly, we found that ~75% of the tailed-piRNAs identified in our anti-MIWI RIP-seq datasets were mono-nucleotide tailed (Fig. 1c), among which mono-uridylation accounts for >90% (Fig. 1d). Similarly, by analyzing previous RIP-seq datasets from wild-type mouse testes (Supplementary information, Table S2), we found that 3′ tailing was detected on ~13.6% of MILI-bound piRNAs and ~14.2% of MIWI2-bound piRNAs (Supplementary information, Fig. S2a), also with mono-nucleotide tailing as the major tailing form (Supplementary information, Fig. S2b). However, in contrast to mono-uridylation tailing predominately on MIWI-bound piRNAs (Fig. 1d), both MILI- and MIWI2-bound piRNAs were equally tailed by uridine (U), adenine (A), and cytosine (C), but weakly by guanosine (G; Supplementary information, Fig. S2c). In line with this, we found that MIWI-bound piRNAs (Fig. 1e), but not MILI- or MIWI2-bound piRNAs (Supplementary information, Fig. S2d), showed a significant U bias at the 3′ end (referred to as -1U preference). Together, these results suggest that 3′ mono-uridylation appears to selectively occur on MIWI-bound piRNAs, implying a functional role for such modification in MIWI/piRNA functions in mouse testes.

We next examined how MIWI-bound piRNAs are uridylated. TUT1, TUT4, and TUT7 are the terminal uridylyl transferases (TUTs) to catalyze RNA uridylation in mammals.[1] Interestingly, a recent study shows a marked decrease in the frequency of 3′ uridylated pachytene piRNAs in *Tut4/7*^{cKO} (*Tut4*$^{fl/fl}$; *Tut7*$^{fl/fl}$; *Stra8-Cre*) pachytene spermatocytes,[6] implying potential roles for TUT4 and TUT7 in piRNA uridylation. To biochemically test whether these TUTs are directly responsible for piRNA uridylation, we first established an in vitro piRNA uridylation assay as described previously,[7] using piR-T (the most abundant mono-uridylated piRNA) and piR-A (the most studied piRNA) as substrates (Supplementary information, Fig. S3a and Table S1). We found that immunopurified Myc-tagged TUT4 and TUT7 but not TUT1 (Supplementary information, Fig. S3b), were able to uridylate piR-T and piR-A in vitro (Fig. 1f, lane 2 vs lanes 3 and 4). Moreover, both TUT4 and TUT7 enhanced piRNA uridylation in a dosage- or time-dependent manner (Supplementary information, Fig. S3c, d), whereas their catalytically dead mutants failed to uridylate piRNAs (Supplementary information, Fig. S3e). These results suggest TUT4/7 as the TUTs for piRNA uridylation. Consistently, by reanalyzing the previous datasets in *Tut4/7*^{cKO} mice[6] using our analysis pipeline, we found that loss of TUT4/7 led to a dramatic reduction of 3′ mono-uridylated piRNAs but barely altered other types of mono-tailed piRNAs in mouse pachytene spermatocytes (Fig. 1g). These results together suggest that TUT4/7 may catalyze piRNA 3′ uridylation in mouse male germ cells.

We next examined the effect of 2′-*O*-methylation at the 3′ end on piRNA uridylation. This modification is known as a hallmark of piRNAs written by HENMT1 in mouse testes.[2,8] Interestingly, we found that both TUT4 and TUT7 were unable to uridylate piRNAs with 2′-*O*-methylation at the 3′ end in vitro (Fig. 1f, lanes 7 and 8), indicating that 2′-*O*-methylation inhibits piRNA uridylation by TUT4/7. We noted a previous report showing that loss of *Henmt1* significantly increases the proportion of piRNAs with uridylation at their 3′ ends in mice.[8] Consistently, reanalysis of the small RNA-seq datasets in *Henmt1* mutant mice[8] by our pipeline confirmed that loss of 2′-*O*-methylation significantly increased piRNA 3′ uridylation

Received: 24 November 2021 Accepted: 29 March 2022
Published online: 15 April 2022

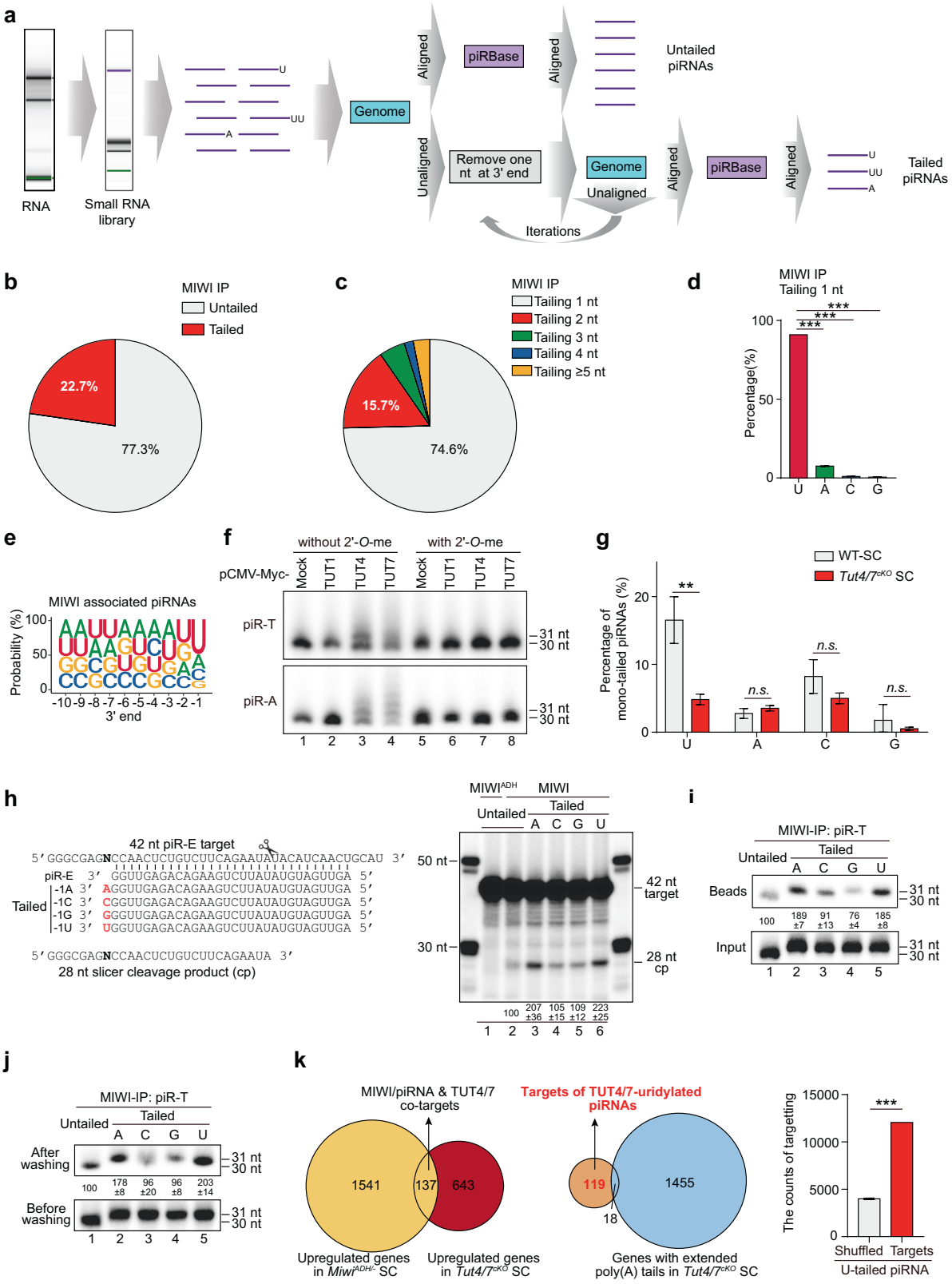

in mouse male germ cells (Supplementary information, Fig. S4a). These results suggest that uridylation tailing on piRNAs might occur before their 2′-*O*-methylation by HENMT1 in mouse testes. To corroborate this, we further analyzed piRNA tailing in $NaIO_4$-treated small RNA-seq datasets generated in our recent study.[9] The 2′-*O*-methylation at the 3′ end of RNAs is known to confer resistance to $NaIO_4$ oxidization. We found that $NaIO_4$ treatment barely altered either the levels or types of 3′ tailing on mouse piRNAs (Supplementary information, Fig. S4b, c), indicating that the tailed-piRNAs possess the 2′-*O*-methylation at the 3′ end. These results together support the notion that piRNA tailing occurs before their 2′-*O*-methylation in mouse testes. Given that mono-uridylation is the

Fig. 1 piRNA 3′ uridylation promotes piRNA binding to MIWI protein and enhances the targeting capacity of MIWI/piRNA in mouse male germ cells. a A schematic diagram illustrating the analysis of untailed- and tailed-piRNAs. **b** Pie chart showing the proportion of tailed- and untailed-piRNAs identified in anti-MIWI RIP-seq from mouse testes. **c** Pie chart showing the proportion of piRNAs tailed by 1–4 nt or ≥5 nt among the tailed piRNAs. **d** Comparison of the proportion of piRNAs tailed respectively by U, A, C, or G among the 1 nt-tailed piRNAs ($n = 2$). **e** MIWI-bound piRNAs show a significant U bias at the 3′ end. The relative nucleotide abundance at each position in the 3′ part of piRNAs is shown. **f** In vitro piRNA uridylation respectively by TUT1 (lanes 2 and 6), TUT4 (lanes 3 and 7) and TUT7 (lanes 4 and 8), using chemically synthesized piR-T (top) and piR-A (bottom) without (lanes 1–4) or with 2′-*O*-methylation (lanes 5–8) as substrates. **g** Mono-uridylated piRNAs, but not mono (A, G, or C)-tailed piRNAs, were significantly reduced in *Tut4/7*^{cKO} spermatocytes compared with wild-type control ($n = 3$). **h** In vitro MIWI slicer assay to examine the effect of piRNA tailing on MIWI-mediated cleavage of target transcript. A [^{32}P]-labeled 42-nt target transcript was incubated with MIWI complexed with untailed piR-E (lane 2) or its mono-tailed paralogs (lanes 3–6), with MIWI^{ADH} mutant complexed with untailed piR-E (lane 1) serving as a negative control. Left, scheme showing the synthetic target ("N" indicated random bases), untailed and tailed piR-E piRNAs and expected 28-nt cleaved product; right, representative image of in vitro MIWI slicer assay. The relative slicer activity is quantified by using the ratio of cleaved product and uncleaved target RNA (the one in wild-type MIWI and untailed piR-E is set as 100%). **i** In vitro MIWI loading assay showing the effect of piRNA tailing on the binding of piRNA to MIWI. [^{32}P]-labeled untailed piR-T and its mono-tailed paralogs were loaded with immunopurified Flag-MIWI protein, with quantification of MIWI-loaded piRNA indicated in parentheses (the one in untailed piR-T normalized with input is set as 100%). **j** piRNA tailed by a U or A, rather than C or G, formed more stable complexes with MIWI than its untailed paralog, with quantification of the remaining MIWI-loaded piRNAs after stringent washing (the one in untailed piR-T is set as 100%). **k** TUT4/7-mediated piRNA uridylation might be involved in regulating a group of target genes in mouse spermatocytes. Left, Venn diagram showing that 137 genes were upregulated in both *Tut4/7*^{cKO} (red) and *Miwi*$^{ADH/-}$ spermatocytes (yellow); middle, Venn diagram showing that 119 out of the 137 upregulated mRNA transcripts do not contain the extended poly(A) tails in *Tut4/7*^{cKO} spermatocytes (blue); right, histogram showing the matched pairs between the 119 target transcripts and uridylated piRNAs using the piRNA-guided cleavage parameters, with the randomly shuffled transcript sequences as negative controls. Results shown in **f**, **h**, **i**, **j** are representative of three independent experiments. $^{**}P < 0.01$, $^{***}P < 0.001$, n.s., not significant.

major tailing form of MIWI-bound piRNAs, we speculate that due to the competition between TUT4/7 and HENMT1, most mono-uridylated piRNAs are immediately methylated by HENMT1, thereby preventing the 3′ tailing from further extension.

We further asked why MIWI-bound piRNAs, rather than MILI- or MIWI2-bound piRNAs, are preferentially uridylated in mouse testes (Fig. 1d; Supplementary information, Fig. S2c). To address this, we examined the interaction between mouse PIWI proteins and TUT4/7. Due to lack of antibodies with appropriate quality for co-immunoprecipitation assay to examine the interaction between endogenous PIWI and TUT proteins in mouse testes, we examined their interactions in co-transfected 293T cells. Interestingly, we found that TUT4/7 significantly interacted with MIWI but barely with MILI or MIWI2, while the interaction between TUT4/7 and MIWI was insensitive to RNase A treatment, suggesting the direct interaction between them (Supplementary information, Fig. S5). These results thus suggest the selective uridylation on MIWI-bound piRNAs likely due to a better interaction between MIWI and TUT4/7.

The selective uridylation on MIWI-bound piRNAs implies a functional requirement of such modification for MIWI/piRNA functions in mouse male germ cells. Previous studies from us and others demonstrate that MIWI/piRNAs function to cleave transposon mRNAs[10] and also play a dual role in regulating protein-coding mRNAs in mouse testes.[11] To experimentally examine the effect of piRNA 3′ uridylation on MIWI/piRNA functions, we first performed in vitro MIWI slicer assays to compare the activity of chemically synthesized piR-E with its paralogs respectively tailed with a A, C, G, or U at the 3′ end (referred to as -1A, -1C, -1G, or -1U, respectively). To rule out potential contribution of extended target complementarity by tailed guide piRNAs, we synthesized the target with random bases at the site corresponding to the tailed nucleotide of guide piRNAs (Supplementary information, Table S3). Intriguingly, we found that U- or A-tailed piR-E, but not the C- or G-tailed, showed an enhanced activity in cleavage of target transcript compared with the untailed control (Fig. 1h). This suggests that addition of a U or A at the 3′ end of guide piRNAs may promote the targeting capacity of MIWI/piRNAs. To corroborate this, we further examined the effect of piRNA tailing on MIWI/piRNA-mediated target gene regulation. Using the target reporter constructs generated in our previous studies,[4,5] we found that U- or A-tailed guide piRNAs, but not the C- or G-tailed, showed an enhanced targeting capacity in both repressing target expression and activating target translation (Supplementary information, Fig. S6). These results together indicate that U or A tailing on guide piRNAs enhances the targeting efficacy of MIWI/piRNAs.

To investigate how 3′ tailing affects the targeting efficacy of MIWI/piRNAs, we first performed in vitro binding assay as descried previously[12] to examine the impact of tailed nucleotides on the assembly of MIWI/piRNA complex. We found that much more U- or A-tailed piR-T, but not the C- or G-tailed, was loaded onto MIWI protein compared with the untailed piR-T (Fig. 1i). Moreover, the MIWI/piRNA complexes formed with -1U or -1A piR-T were more stable under harsh washing (Fig. 1j). These results indicate that MIWI shows a better binding capacity for -1U or -1A piRNAs. Consistent with this observation, we found that increasing guide piRNA expression effectively compensated the targeting deficiency of -1C, -1G, or untailed guide piRNAs (Supplementary information, Fig. S6). Additionally, although MIWI showed binding preference to both -1U and -1A piRNAs in vitro, endogenous MIWI-bound piRNAs exhibit a significant -1U bias in mouse testes (Fig. 1e). We reasoned that this is likely due to MIWI-bound piRNAs preferentially undergoing 3′ uridylation in vivo, given the direct interaction between MIWI and TUT4/7 (Supplementary information, Fig. S5). Collectively, these results suggest that piRNA 3′ uridylation facilitates the assembly of MIWI/piRNA complex, thereby reinforcing MIWI/piRNA functions in mouse male germ cells.

Finally, we sought to explore the biological roles of piRNA 3′ uridylation in mouse testes. The MIWI/piRNA machinery has been shown to play its roles in a developmental stage-specific manner.[4,5,13,14] *Tut4/7*^{cKO} mice show spermatogenic arrest in late pachytene stage, preventing us from determining the role of TUT4/7-mediated piRNA 3′ uridylation during spermiogenesis using the existing genetic model. We thus analyzed the effect of TUT4/7-mediated piRNA 3′ uridylation on MIWI/piRNA slicer activity during meiosis using previous *Tut4/7*^{cKO} spermatocyte transcriptomes[6] and our newly generated *Miwi*$^{ADH/-}$ spermatocyte transcriptomes. Cross analysis revealed that 137 mRNA transcripts are significantly elevated in both *Tut4/7*^{cKO} and *Miwi*$^{ADH/-}$ spermatocytes, suggesting this group of genes as the co-targets of MIWI/piRNAs and TUT4/7 (Fig. 1k, left). Given that TUT4/7 also act to prime mRNA 3′ uridylation and degradation, we employed the TAIL-seq datasets of *Tut4/7*^{cKO} spermatocytes[6] to exclude the direct targets by TUT4/7-primed mRNA 3′ uridylation. We found that 119 out of the 137 MIWI/piRNA and TUT4/7 co-target transcripts did not show any extended tails (Fig. 1k, middle; Supplementary information, Table S4), among which >30 mRNA transcripts have been previously validated as MIWI/piRNA-cleaved targets,[13–15] including *Ppp1cb*, *Golga2*, *zyg11b*, and *Stambp* (Supplementary information, Fig. S7a). Using the piRNA-guided

cleavage parameters,[13] we found that this group of mRNAs was readily matched to the uridylated piRNAs, further suggesting them as the direct targets of TUT4/7-uridylated piRNAs (Fig. 1k, right). Gene Ontology analysis showed that these direct target genes are involved in several biological events in meiosis/mitosis, such as microtubule dynamics (polymerization and depolymerization) and DNA replication checkpoint (Supplementary information, Fig. S7b). These results together suggest that TUT4/7-primed piRNA 3′ uridylation is responsible for the degradation of a subset of mRNA transcripts in mouse spermatocytes.

In summary, we show the presence of 3′ tailing on mature piRNAs in mouse testes and further identified TUT4/7-primed uridylation as the major tailing form on MIWI-bound piRNAs. Moreover, our data suggest that 3′ tailing on piRNAs likely occurs between pre-piRNA trimming by PNLDC1 and 2′-*O*-methylation by HENMT1 (Supplementary information, Fig. S8). Importantly, our findings show that 3′ uridylation contributes to the targeting capacity of MIWI/piRNAs, mirroring the requirement of MIWI/piRNA functions for post-transcriptional regulation of protein-coding mRNAs during mouse spermatogenesis. Collectively, these findings demonstrate the functional importance of 3′ uridylation for MIWI/piRNA functions in male germ cells, uncovering an unprecedented role for 3′ tailing in piRNA biology. It will be interesting to determine whether and how such modification on MILI- and MIWI2-bound piRNAs plays any role in future studies.

Mao-Zhou Zhao[1,4], Di-Hang Lin[1,4], Heng Zuo[1,4], Huan Wei[2], Xin Wang[1,2✉], Lan-Tao Gou[1✉] and Mo-Fang Liu[1,2,3✉]

[1]State Key Laboratory of Molecular Biology, State Key Laboratory of Cell Biology, Shanghai Key Laboratory of Molecular Andrology, Shanghai Institute of Biochemistry and Cell Biology, Center for Excellence in Molecular Cell Science, Chinese Academy of Sciences; University of Chinese Academy of Sciences, Shanghai, China. [2]School of Life Science, Hangzhou Institute for Advanced Study, University of Chinese Academy of Sciences, Hangzhou, Zhejiang, China. [3]School of Life Science and Technology, Shanghai Tech University, Shanghai, China. [4]These authors contributed equally: Mao-Zhou Zhao, Di-Hang Lin, Heng Zuo. ✉email: wx@ucas.ac.cn; goulantao@sibcb.ac.cn; mfliu@sibcb.ac.cn

REFERENCES

1. Liudkovska, V. & Dziembowski, A. *Wiley Interdiscip. Rev. RNA* **12**, e1622 (2021).
2. Ozata, D. M., Gainetdinov, I., Zoch, A., O'Carroll, D. & Zamore, P. D. *Nat. Rev. Genet.* **20**, 89–108 (2019).
3. Pastore, B., Hertz, H. L., Price, I. F. & Tang, W. *Cell Rep.* **36**, 109640 (2021).
4. Dai, P. et al. *Cell* **179**, 1566–1581 (2019).
5. Gou, L. T. et al. *Cell Res.* **24**, 680–700 (2014).
6. Morgan, M. et al. *Cell Res.* **29**, 221–232 (2019).
7. Heo, I. et al. *Cell* **151**, 521–532 (2012).
8. Lim, S. L. et al. *PLoS Genet.* **11**, e1005620 (2015).
9. Li, F. et al. *Nat. Cell Biol.* **22**, 425–438 (2020).
10. Reuter, M. et al. *Nature* **480**, 264–267 (2011).
11. Dai, P., Wang, X. & Liu, M. F. *Sci. China Life Sci.* **63**, 447–449 (2020).
12. Kawaoka, S., Izumi, N., Katsuma, S. & Tomari, Y. *Mol. Cell* **43**, 1015–1022 (2011).
13. Goh, W. S. et al. *Genes Dev.* **29**, 1032–1044 (2015).
14. Watanabe, T., Cheng, E. C., Zhong, M. & Lin, H. *Genome Res.* **25**, 368–380 (2015).
15. Zhang, P. et al. *Cell Res.* **25**, 193–207 (2015).

ACKNOWLEDGEMENTS

We thank members of the M.-F.L. lab and L.-T.G. lab for helpful comments. We thank Drs Marcos Morgan and Dónal O'Carroll from University of Edinburgh for the TAIL-seq datasets of *Tut4/7*^{cKO} spermatocytes. This work was supported by the National Key R&D Program of China (2017YFA0504400, and 2021YFC2700200), the Strategic Priority Research Program of the Chinese Academy of Sciences (XDB19010203), the National Natural Science Foundation of China (91940305, 31830109, 31821004, 31961133022, 91640201, 32170815 and 32101037), Science and Technology Commission of Shanghai Municipality (17JC1420100, 2017SHZDZX01, 19JC1410200, 21PJ1413800, 21ZR1470200, 21YF1452700 and 21ZR1470500), China Postdoctoral Science Foundation (2020T130670 and 2020M671256) and the Foundation of Key Laboratory of Gene Engineering of the Ministry of Education.

AUTHOR CONTRIBUTIONS

X.W., L.-T.G., and M.-F.L. planned the project. M.-Z.Z., D.-H.L, X.W., L.-T.G., and M.-F.L. designed the experiments. M.-Z.Z., D.-H.L, and X.W. conducted the experiments. H.Z., H.W., and X.W. analyzed the data. X.W., L.-T.G., and M.-F.L. wrote the manuscript.

COMPETING INTERESTS

The authors declare no competing interests.

ADDITIONAL INFORMATION

Supplementary information The online version contains supplementary material available at https://doi.org/10.1038/s41422-022-00659-1.

Correspondence and requests for materials should be addressed to Xin Wang, Lan-Tao Gou or Mo-Fang Liu.

Reprints and permission information is available at http://www.nature.com/reprints